The sulfur budget of the 2011 Grímsvötn eruption, Iceland

Olgeir Sigmarsson[1,2], Baptiste Haddadi[1], Simon Carn[3], Séverine Moune[1], Jónas Gudnason[2], Kai Yang[4,5] and Lieven Clarisse[6]

[1]LMV, CNRS-UBP-IRD, 5 rue Kessler, 63038 Clermont-Ferrand, France

[2]ISE, University of Iceland, 101 Reykjavik, Iceland

[3]Dept Geo Min Eng Sci, MTU, 1400 Townsend Drive, Houghton, MI 49931, USA

[4]Atmospheric Chemistry and Dynamics Laboratory, Code 614, NASA Goddard Space Flight Center, 8800 Greenbelt Rd Greenbelt, MD 20771, USA

[5]Dept of Atmospheric and Oceanic Science, University of Maryland College Park, College Park, MD 20742, USA

[6] Spectroscopie de l'Atmosphère, Service de Chimie Quantique et Photophysique, Université Libre de Bruxelles, Brussels, Belgium

e-mails: olgeir@opgc.univ-bpclermont.fr, b.haddadi@opgc.univ-bpclermont.fr , scarn@mtu.edu, s.moune@opgc.univ-bpclermont.fr, jog4@hi.is, kai.yang-1@nasa.gov, lclariss@ulb.ac.be

Key points

- H_2S and SO_2 degassing is estimated for the 2011 eruption of Grímsvötn

- Satellite-based sulfur mass loading is lower than from mineral melt-inclusions

- Half of S resides as sulfide globules; 25% enter the stratosphere
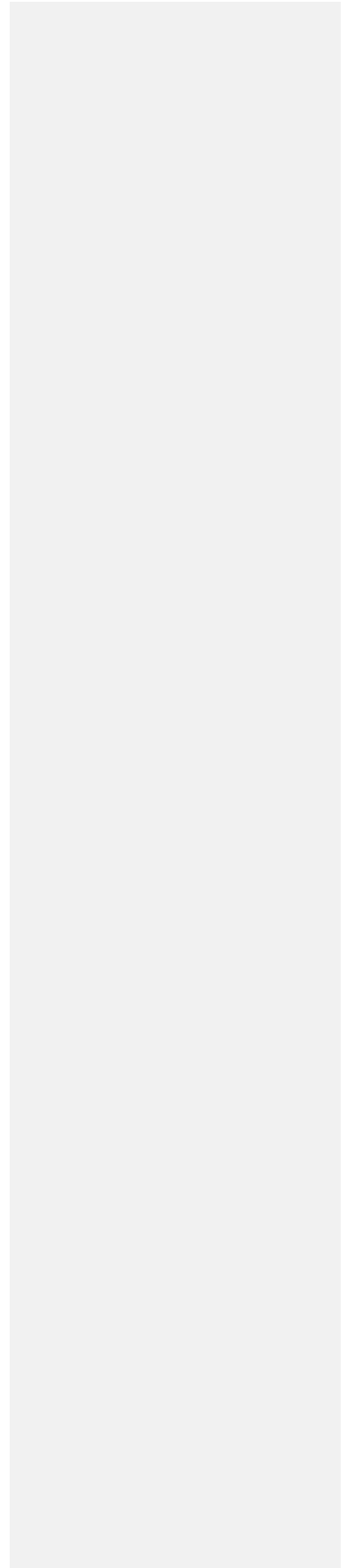
Sulfur concentrations have been measured in twenty eight melt inclusions (MI) in plagioclase, clinopyroxene and olivine crystals extracted from tephra produced during the explosive eruption of Grímsvötn in May 2011. The results are compared to sulfur concentrations in the groundmass glass in order to estimate the mass of sulfur brought to surface during the eruption. Satellite measurements yield order of magnitude lower sulfur (~0.2 Tg) in the eruption plume than estimated from the difference between MI and the groundmass glass. This sulfur "deficit" is readily explained by sulfur adhering to tephra grains but principally by sulfide globules caused by basalt-sulfide melt exsolution before degassing. A mass-balance calculation reveals that approximately ~0.8 Tg of SO_2 is present as globules, representing ~50% of the total sulfur budget. Most of the sulfide globules likely reside at depth due their elevated density, for potential later remobilization by new magma or hydrothermal circulation.

Index term: 8137 Hotspots, large igneous provinces, and flood basalt volcanism, 8410 Geochemical modeling (1009, 3610), 8430 Volcanic gases, 8428 Explosive volcanism (4302), 8485 Remote sensing of volcanoes (4337)

1. Introduction

Sulfur degassing from hot-spot related volcanoes is an important contribution to the total mass loading of the atmosphere [e.g. Wallace, 2001]. The mass loading of sulfur can be estimated directly from satellite measurements of sulfur dioxide in the eruptive plume, or indirectly from the difference in sulfur concentrations in pristine melt inclusions (MI) and outgassed groundmass glass (the so-called petrologic method; Devine et al., 1984). The sulfur budget at volcanoes from subduction-zone settings is often underestimated by the petrologic

method but at hot-spot related volcanoes, a relatively good agreement has been found from both methods [e.g. Sharma et al., 2004; Moune et al., 2007]. An excellent opportunity to test the consistency between these two methods came during the 2011 eruption of Grímsvötn volcano, Iceland.

## 2.	The 2011 Grímsvötn eruption

Grímsvötn is the most active volcano in Iceland, located beneath the Vatnajökull ice-sheet. A sub-glacial caldera lake is maintained by extensive geothermal activity leading to periodic water outburst floods, or jökulhlaups that may empty the lake. The resulting pressure release is often followed by a small eruption such as the November 2004 eruption, which produced 0.02 km^3 DRE (Dense Rock Equivalent) volume of basaltic tephra [e.g. Thorarinsson, 1974; Albino et al., 2010; Jude-Eton et al., 2012]. The 2011 eruption began at 19 UTC on 21 May. The plume quickly rose to 20-25 km [Petersen et al., 2012] impacting aviation in Northern Europe. The eruption ended on May 28 having produced an order of magnitude larger volume of magma than in 2004, or approximately 0.2-0.3 km^3 DRE, with tephra fallout detected outside Iceland in Jan Mayen, the British Isles and Scandinavia [Gudmundsson et al., 2012]. Most of the magma was erupted during the first two days and its composition was uniform, namely a quartz-normative tholeiitic basalt typical of the last 7000 years of activity at Grímsvötn [Óladóttir et al., 2011a]. It has sparse phenocrysts of plagioclase (plag), clinopyroxene (cpx) and olivine (ol) in decreasing order of abundance. The ubiquitous presence of magnetite and rare occurrence of sulfide globules in the 2011 tephra are observed here for the first time in Grímsvötn deposits (Fig. 1).

Four fine-grained tephra samples were collected during the eruption on the lowland 45-75 km south of the volcano (three samples collected at different localities on a transect through the tephra fall sector (Gv1-3) during the first eruption night and a bulk sample representing the first four days of the eruption (Gv4)). In addition, near-vent lapilli-sized tephra from the first eruption day was later sampled on the caldera rim 1 km south of the eruption site (sample Gv2011-D). The 2011 tephra is composed of glass (95-99 %) with only 1-5 % of visible crystals.

3.   Analytical methods and results

3.1 Petrologic estimate of S degassing

Olivine, cpx and plag crystals were handpicked under a binocular microscope from the 100-250 and 250-600 µm grain-size fractions of crushed tephra. Crystals with MI were washed with acetone, embedded in epoxy and polished individually to generate adequate exposure of the MI for in-situ electron probe microanalysis. The MI are spherical to oblate in shape and range in size from 5 to 190 µm. Most MI contain shrinkage bubbles but all are totally deprived of daughter minerals. In total 19 crystals containing 28 MI were selected and prepared for analysis. The number of host crystals with MI reflects the relative abundance in the phenocryst assemblage; 21 MI in 13 plag, 6 in 5 cpx and a single one in an ol. The groundmass is composed of glass patches with variable microlite contents ranging from those that are completely free of microlites to heavily crystallized groundmass.

Major element and sulfur concentrations were measured on a Cameca SX-100 microprobe at Laboratoire Magmas et Volcans in Clermont-Ferrand, France. The results are given in Table A1 of auxiliary material and analytical details and uncertainties are listed in Óladóttir et al.

[2011b] and Moune et al. [2012]. The largest MI were analyzed with a spot diameter of 20 µm and sample current of 8 nA whereas the three smallest MI were analyzed with a beam of only 1 µm and a current as low as 2 nA. Most MI are of basaltic composition, but three basaltic icelandite compositions are observed as well. The groundmass glass composition is comparable to that of other Grímsvötn tephra.

Sulfur concentrations in the MI vary from 1311 to 1982 ppm (Table A1) whereas lower values are measured in the groundmass glass (449 to 895 ppm; mean = 651±52 (2SE) ppm; 26 glass grains; Table A2). The microlite-free glass has higher S concentrations than those that are rich in microlites, suggesting degassing-induced crystallization. The S concentrations in the MI exceed the sulfide saturation curve of submarine MORB glasses [e.g. Wallace and Edmonds, 2011] in accordance with the presence of sulfide globules in Grímsvötn 2011 tephra (Fig. 1c). Sulfide saturation and known sulfur content at sulfide saturation level in basalts [SCSS; Jugo, 2012] suggest that the Grímsvötn magma has oxygen fugacity close to FMQ.

3.2 Satellite-based SO_2 and H_2S measurements

We use ultraviolet (UV) measurements from the Ozone Monitoring Instrument (OMI) aboard NASA's polar-orbiting Aura satellite to quantify SO_2 emissions during the 2011 Grímsvötn eruption. Although OMI data are currently impacted by a sensor anomaly that reduces the spatial coverage of the sensor [Carn et al., 2013], the high latitude of Grímsvötn mitigated this by providing numerous overlapping OMI orbits that covered the SO_2 cloud. The eruption began late in the afternoon of May 21, and the first complete coverage of the eruption cloud by OMI (daytime only) occurred on May 22 at ~11:50 UTC. A notable feature of the eruption was a distinct separation of the SO_2- and ash-rich portions of the volcanic cloud (Fig. 3), with

the ash cloud advected south and then east of Grímsvötn at lower altitudes, whilst the stratospheric SO_2 drifted north.

Operational OMI SO_2 retrievals using the linear fit (LF) algorithm [Yang et al., 2007], assuming a lower stratospheric altitude (note that the precise SO_2 altitude has little impact on SO_2 loading above ~10 km), detected ~0.2 Tg of SO_2 in the eruption cloud on May 22. Errors on SO_2 retrievals are estimated to be ~20%. A peak SO_2 loading of ~0.3 Tg was measured by OMI on May 23 when the volcanic cloud had spread over eastern Greenland and the Greenland Sea. In order to exclude the potential underestimation of large SO_2 column amounts by the LF algorithm, we also analyzed Extended Iterative Spectral Fit (EISF) retrievals [Yang et al., 2010] for the Grímsvötn plume. The EISF measurements were commensurate with the LF results, providing confidence in the calculated SO_2 loadings. The SO_2 loading gradually decayed after May 23, with remnants of the stratospheric SO_2 cloud detected by OMI until early June. We estimate an e-folding time of ~10-15 days for the stratospheric SO_2, and extrapolation of the daily SO_2 loadings back to the eruption time yields an initial SO_2 mass within the 20% error on the peak measured value of 0.3 Tg. The SO_2 emissions during the 2011 eruption of Grímsvötn were around an order of magnitude higher than those measured by OMI during its November 2004 eruption, which concurs with the different magma volumes erupted.

Other potentially significant sulfur species in divergent-plate volcanic gases are H_2S and S_2 [Symonds et al., 1994]. The latter is not measurable using remote sensing techniques, but to assess H_2S emissions from Grímsvötn we use satellite data from the Infrared Atmospheric Sounding Interferometer (IASI) aboard MetOp-A [Clarisse et al., 2011]. IASI measured a maximum of 29 Gg of H_2S on May 22, collocated with the SO_2 cloud; this is only the second reported satellite-based detection of H_2S in a volcanic plume after the 2008 Kasatochi eruption [Clarisse et al., 2011]. IASI also measured ~0.3 Tg of SO_2 in the

Grímsvötn volcanic cloud, corroborating the OMI data. This yields a H_2S/SO_2 mass ratio of ~0.1, which is similar to average ratios reported for directly sampled rift volcanic gases derived from tholeiitic basalts [0.06; Symonds et al., 1994]. Based on this concurrence, we use reported S_2/SO_2 ratios [Symonds et al., 1994] to estimate a maximum S_2 loading of ~15 Gg. Hence the total estimated sulfur loading based on satellite data is 150 Gg (as SO_2) + 27 Gg (as H_2S) + 15 Gg (as S_2) = 0.192 Tg S.

Textor et al. [2003] modeled scavenging of volcanic gases on hydrometeor-ash aggregates in eruption columns, concluding that 80% of sulfur gases (SO_2 and H_2S) would reach the stratosphere. Olsson et al. [2013] have estimated from leaching experiments on freshly fallen 2011 Grímsvötn tephra that approximately 118 Gg of S was sequestered on the volcanic ash during the eruption. In conjunction with the satellite measurements, this implies that a total of 0.31 Tg of S was emitted during the 2011 Grímsvötn eruption, of which 0.192 Tg reached the stratosphere and 0.118 Tg (~38%) was scavenged in the eruption column. We suggest that this high scavenging efficiency (38% cf. 20% estimated by Textor et al., 2003) reflects the wet nature of the sub-glacial Grímsvötn eruption, with abundant hydrometeors.

4.   Discussion

The sulfur concentration in the melt before degassing can be estimated from the measured concentration in the MI. The regular increase in K_2O, with decreasing MgO content in the groundmass glass (Fig. 2a), permits assessment of the significance of the S concentrations in the different MI. These variable S concentrations reflect, in part, host crystallization of the initial MI. Such crystallization can be readily corrected for olivine, which has a well-defined equilibrium K_D of Fe and Mg exchange between melt and crystal [e.g. Roeder and Emslie, 1970]. Corrections for cpx and plag crystallization are less straightforward. Therefore, we use

the relationship between two incompatible elements in plag, namely K_2O and MgO (Fig. 2a). The MI forming a linear correlation extrapolated from the origin, are clearly affected by plag host crystallization. Other MI in plag that have significantly higher MgO and K_2O than the groundmass glass may have also experienced host crystallization. The plag MI (G1-D1) with abnormally high MgO and lowest S concentration is clearly an outlier; possibly a xenocryst in the 2011 magma. By the same token, the cpx MI with the lowest MgO concentration lying on a vector extrapolated from the concentrations measured in the ferromagnesian minerals (cpx and ol with respectively, MgO and K_2O concentrations equal to 17.4; 0.02 and 37.5; 0%), may have been affected by host crystallization as well. The initial S concentration in the magma thus appears best represented by the relatively primitive cpx MI with 8 > MgO > 6%. We note that these MI lie at the low K_2O and high MgO end of the differentiation trend of the groundmass composition as expected for a parental magma composition for Grímsvötn. These two MI have K_2O values close to 0.4% whereas the degassed groundmass glass has average K_2O of 0.5%. We have therefore corrected their S concentration for 20% fractional crystallization (needed to explain K_2O increase from 0.4 to 0.5%; see Moune et al., 2007) to obtain an initial S concentration ($S_{initial}$) of 1750 ($\pm$ 125; 2σ) ppm (Fig. 2b). A plag MI that plots close to these two cpx MI has sulfur concentration of 1772 ($\pm$ 58; 2σ) ppm that is indistinguishable from our $S_{initial}$ estimate. It is worth noting that this selective choice of MI does not affect the outcome of this paper since the average composition of all MI in cpx yields an initial S concentration less than 10 % lower (X=1558 ($\pm$ 440; 2σ) ppm instead of estimated 1750 ($\pm$ 125; 2σ) ppm), which is within the error of our approach.

The mass of sulfur exsolved from the initial magma can be estimated as follows (the petrologic method; Table 1): mass $SO_2 = \alpha \; \rho \; V_{DRE} \; (S_{initial} - S_{groundmass})$; where $\alpha = MW(SO_2)/MW(S) = 64.06/32.06$, $\rho = 2750$ kg.m^{-3} [McBirney, 2006] and $V_{DRE} = 0.25$ km^3.

This yields 1.47±0.37 Tg (2σ) that is an order of magnitude larger than the sulfur loading from the satellite data. The considerably lower S concentrations in the groundmass glass relative to the MI thus cannot be explained by S degassing only. Presence of sulfide globules demonstrates that sulfide saturation had been reached, which therefore present a sulfur sink. In addition, ~118 Gg of S adhered to the tephra in the eruption column, whilst residual magma from the 2004 eruption (erupted in 2011) may have lost part of its sulfur to the hydrothermal system and the caldera lake. Ágústsdóttir and Brantley [1994] estimated a steady-state sulfur flux of 5.33 x 10^6 kg/year from Grímsvötn's lake composition and volumes of jökulhlaups, which gives 37 Gg over the 7 years repose period preceding the 2011 eruption. The mass balance for the S budget in the Grímsvötn 2011 eruption is thus: $S_{initial} - (S_{groundmass\ glass} + S_{satellite} + S_{leachate} + S_{lake} + S_{sulfide\ globule}) = 0$. Input values and associated errors are listed in Table 1 together with average, minimum and maximum proportions of each sulfur-budget component.

On average, 16% of the sulfur adheres to the tephra glass, 26% are degassed as sulfur, 5% were lost to the lake and 53% of the S is conserved as sulfide globules. The sulfide globules will form a sink at depth due to their elevated density as is observed in cumulate nodules from Piton de la Fournaise, Réunion Island [Collins et al., 2012]. These sulfides may be subsequently remobilized by incoming fresh basaltic magma, undersaturated in sulfide, possibly via reactions such as $\frac{1}{2}$ O_2 (gas) + FeS (sulfide) = FeO (silicate melt) + $\frac{1}{2}$ S_2 (gas). Alternatively, a possible sulfur ore deposit will react with hydrothermal solutions having variable fO_2/fS_2 during the heat mining of basaltic intrusions beneath the geothermal system that maintains the sub-glacial lake at Grímsvötn.

5.   Conclusion

The sulfur budget for the 2011 Grímsvötn eruption cannot be simply treated as initial S in MI minus residual S in groundmass equals sulfur released in a gas phase. We propose that 50% of the sulfur was retained in an immiscible sulfide phase (globules) at depth. In such cases, remotely measured sulfur emissions will only account for the minimum quantity of sulfur brought to the surface in an explosive eruption.

References

Ágústsdóttir, A.M., and S.L. Brantley (1994), Volatile fluxes integrated over four decades at Grímsvötn volcano, Iceland. *J. Geophys. Res., 99*, B5, 9505-9522, doi: 0148-0227/94/93JB-03597$05.00.

Albino, F., V. Pinel, and F. Sigmundsson (2010), Influence of surface load variations on eruption likelihood: application to two Icelandic subglacial volcanoes, Grímsvötn and Katla, *Geophysical Journal International, 181*, 1510-1524, doi: 10.1111/j.1365-246X.2010.04603.x.

Carn, S.A., N.A. Krotkov, K. Yang, and A.J. Krueger (2013), Measuring global volcanic degassing with the Ozone Monitoring Instrument (OMI), In: Pyle, D.M., Mather, T.A. and Biggs, J. (eds) Remote Sensing of Volcanoes and Volcanic Processes: Integrating Observation and Modeling, Geol. Soc. Lon, Special Publications, 380,doi: 10.1144/SP380.12.

Clarisse, L., P.-F. Coheur, S. Chefdeville, J.-L. Lacour, D. Hurtmans, and C. Clerbaux (2011), Infrared satellite observations of hydrogen sulfide in the volcanic plume of the August 2008 Kasatochi eruption, *Geophys. Res. Lett., 38*, L10804, doi: 10.1029/2011GL047402.

Collins, S.J., J. Maclennan , D.M. Pyle , S.J. Barnes, B.G.J. Upton (2012) Two phases of sulphide saturation in Réunion magmas: Evidence from cumulates, *Earth Planet. Sci. Lett., 337–338*,104–113

Devine, J.D., H. Sigurdsson, A.N. Davis and S. Self (1984) Estimates of sulfur and chlorine yield to the atmosphere from volcanic eruptions and potential climatic effects, *J. Geophys. Res. 89,* 6309–6325; DOI: 10.1029/JB089iB07p06309.

Gudmundsson, M. T., Á. Höskuldsson, G. Larsen, T. Thordarson, B. A. Oladottir, B. Oddsson, J. Gudnason, T. Högnadottir, J. A. Stevenson, B. F. Houghton, D. McGarvie, and

G. M. Sigurdardottir (2012), The May 2011 eruption of Grímsvötn , *Geophys. Res. Abstr., 14*, EGU2012-12119.

Jugo, P. J. (2012) Sulfur content at sulphide saturation in oxidized magma, *Geology, 37,* 415-418, doi: 10.1130/G25527A.1

Jude-Eton, T. C., T. Thordarson, M. T. Gudmundsson, and B. Oddsson (2012), Dynamics, stratigraphy and proximal dispersal of supraglacial tephra during the ice-confined 2004 eruption at Grímsvötn Volcano, Iceland, *Bull. Volcanol., 74*, 1057–1082, doi: 10.1007/s00445-012-0583-3

McBirney, A.R. (2006), *Igneous Petrology, Third edition,* Jones and Bartlett, Sudbury, MA, 550 p. ISBN: 9780763734480.

Moune, S., O. Sigmarsson, T. Thordarson, and P.-J. Gauthier (2007), Recent volatile evolution in the magmatic system of Hekla volcano, Iceland, *Earth Planet. Sci. Lett., 255*, 373–389, doi: 10.1016/j.epsl.2006.12.024.

Moune, S., O. Sigmarsson, T. Thordarson, P. Schiano, and J. K. Keiding (2012), Melt inclusion constraints on the magma source of Eyjafjallajökull 2010 flank eruption, *J. Geophys. Res., 117*, B00C07, doi: 10.1029/2011JB008718.

Óladóttir, B., G. Larsen, and O. Sigmarsson (2011a), Holocene volcanic activity at Grímsvötn, Bárdarbunga and Kverkfjöll subglacial centres beneath Vatnajökull, Iceland, *Bull. Volcanol., 73*, 1187–1208, doi: 10.1007/s00445-011-0461-4

Óladóttir, B., O. Sigmarsson, G. Larsen, and J.-L Devidal (2011b), Provenance of basaltic tephra from Vatnajökull subglacial volcanoes, Iceland, as determined by major- and trace-element analyses, *Holocene, 21*, 1037-1048, doi: 10.1177/0959683611400456.

Olsson, J., S. L. S. Stipp, K. N. Dalby and S. R. Gislason (2013), Rapid release of metal salts and nutrients from the 2011 Grímsvötn, Iceland volcanic ash. *Geochim. Cosmochim. Acta, 123*, 134–149, doi: http://dx.doi.org/10.1016/j.gca.2013.09.009

Petersen, G. N., H. Bjornsson, P. Arason, and S. von Löwis (2012), Two weather radar time series of the altitude of the volcanic plume during the May 2011 eruption of Grímsvötn, Iceland, *Earth Syst. Sci. Data, 4*, 121–127, doi: 10.5194/essd-4-121-2012.

Roeder, P. L., and R. F. Emslie (1970), Olivine-liquid equilibrium, *Contrib.Mineral. Petrol., 29*, 275–289, doi: 10.1007/BF00371276.

Sharma, K., S. Blake, S. Self, and A. J. Krueger (2004), SO_2 emissions from basaltic eruptions, and the excess sulfur issue, *Geophy.s Res. Lett., 31,* L13612, doi: 10.1029/2004GL019688.

Symonds, R.B., W.I. Rose, G.J.S. Bluth, T.M. Gerlach (1994), Volcanic-gas studies: methods, results and applications, In: M.R. Carroll and J.R. Holloway (eds), Volatiles in Magmas, *Rev. Mineral.*, *30,* pp. 1-66.

Textor, C., H.-F. Graf, M. Herzog, and J. M. Oberhuber (2003), Injection of gases into the stratosphere by explosive volcanic eruptions, *J. Geophys. Res.*, *108(D19)*, 4606, doi: 10.1029/2002JD002987.

Thorarinsson, S. (1974), *Vötnin stríð. Saga Skeiðarárhlaupa og Grímsvatnagosa* (The swift flowing rivers. Annals of jökulhlaups in the river Skeidará and eruptions of Grímsvötn), Bókútáfa Menningarsjóðs, 254 pp., Reykjavik, Iceland.

Wallace, P. (2001), Volcanic SO_2 emissions and the abundance and distribution of exsolved gas in magma bodies, *J. Volcanol. Geotherm. Res., 108*, 85-106.

Wallace, P. J., and M. Edmonds (2011), The sulfur budget in magmas: Evidence from Melt Inclusions, submarine glasses, and volcanic gas emissions, *Rev. Min. Geochem., 73*, 215-246, 10.2138/rmg.2011.73.8.

Yang, K., N.A. Krotkov, A.J. Krueger, S.A. Carn, P.K. Bhartia, and P.F. Levelt (2007). Retrieval of large volcanic SO_2 columns from the Aura Ozone Monitoring Instrument (OMI): comparison and limitations. *J. Geophys. Res.*, 112, D24S43, doi: 10.1029/2007JD008825.

Yang, K., X. Liu, P.K. Bhartia, N.A. Krotkov, S.A. Carn, E. Hughes, A.J. Krueger, R. Spurr and S. Trahan (2010). Direct Retrieval of Sulfur Dioxide Amount and Altitude from Spaceborne Hyper-spectral UV Measurements: Theory and Application, *J. Geophys. Res.*, 115, D00L09, doi: 10.1029/2010JD013982.
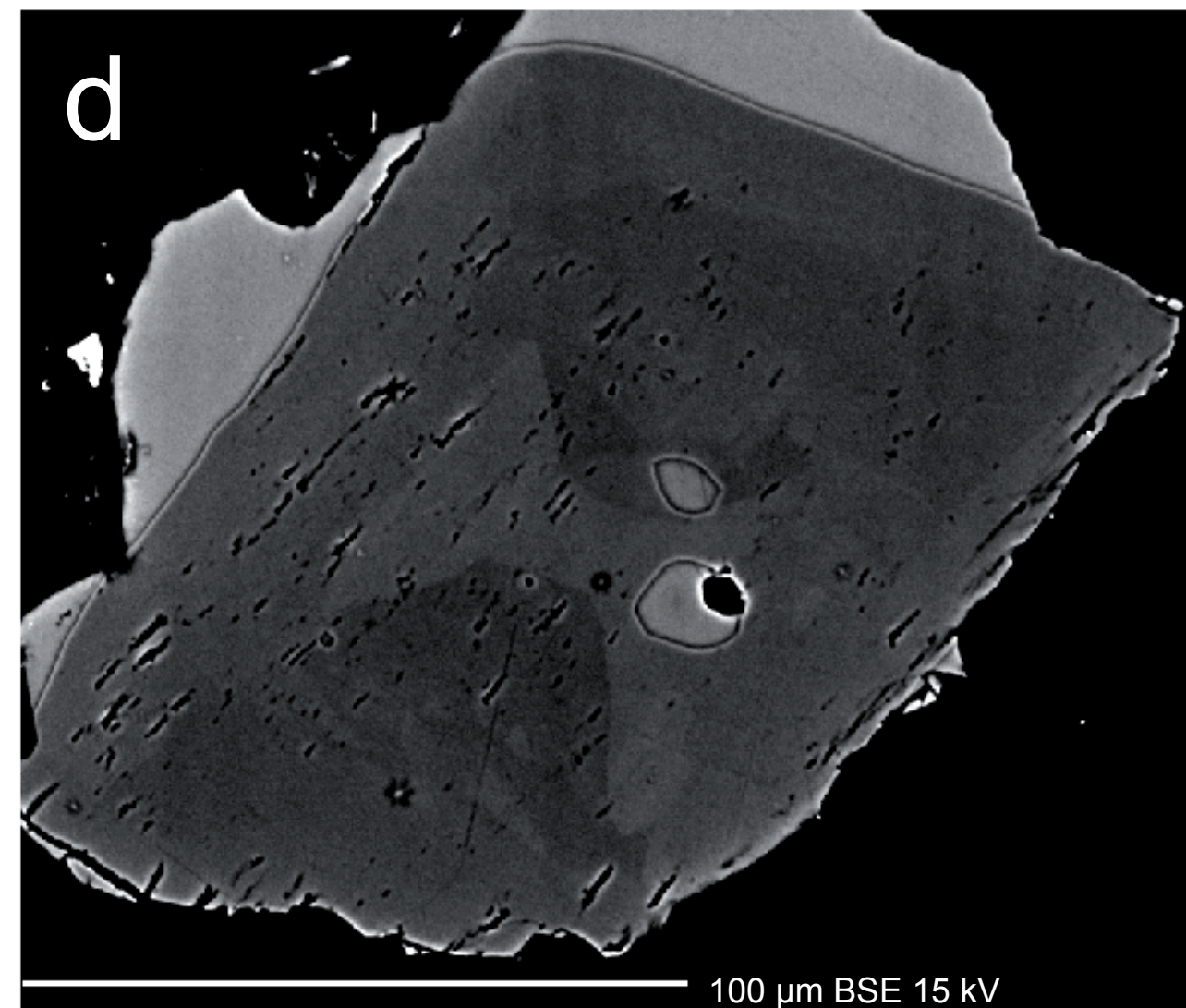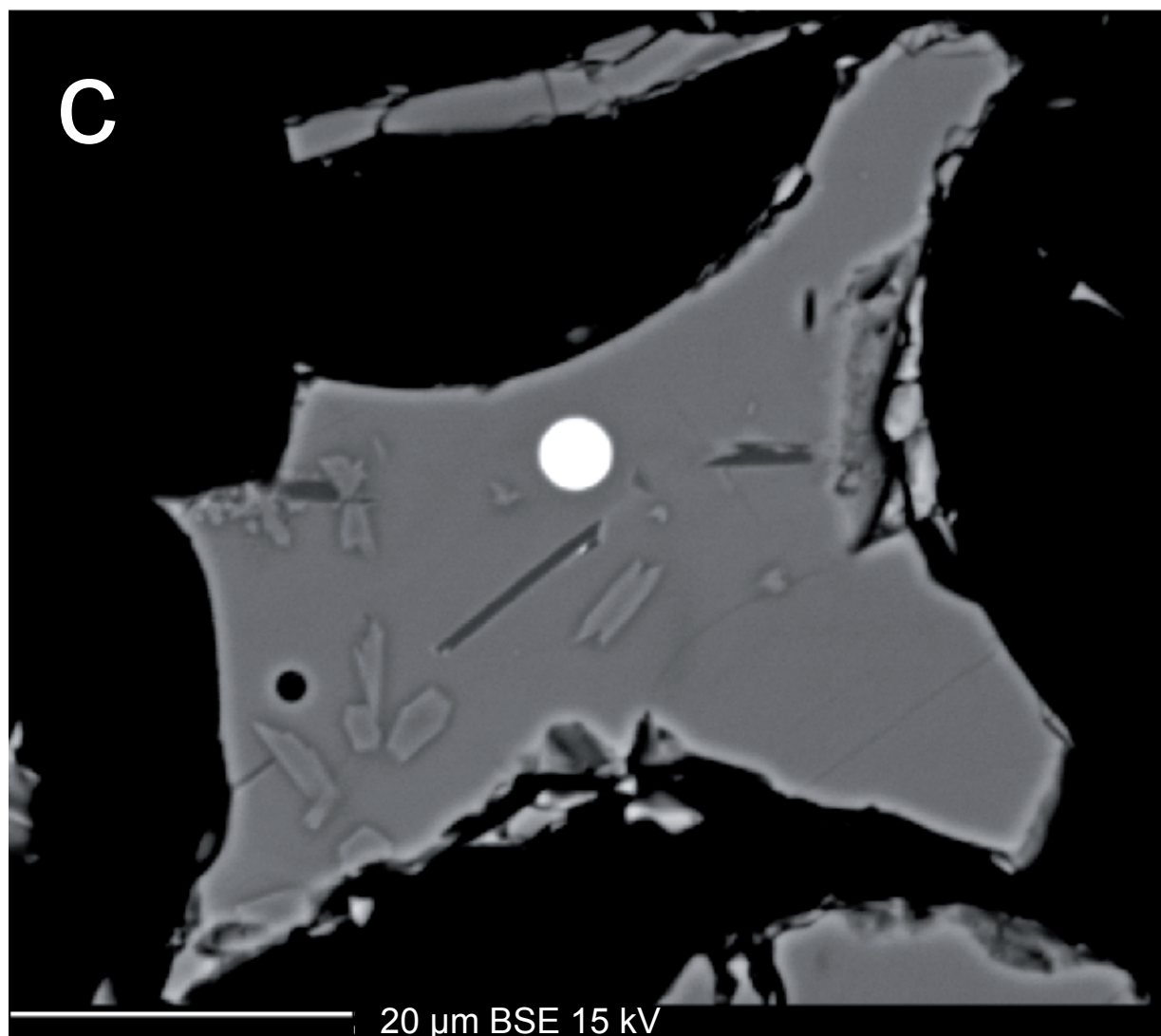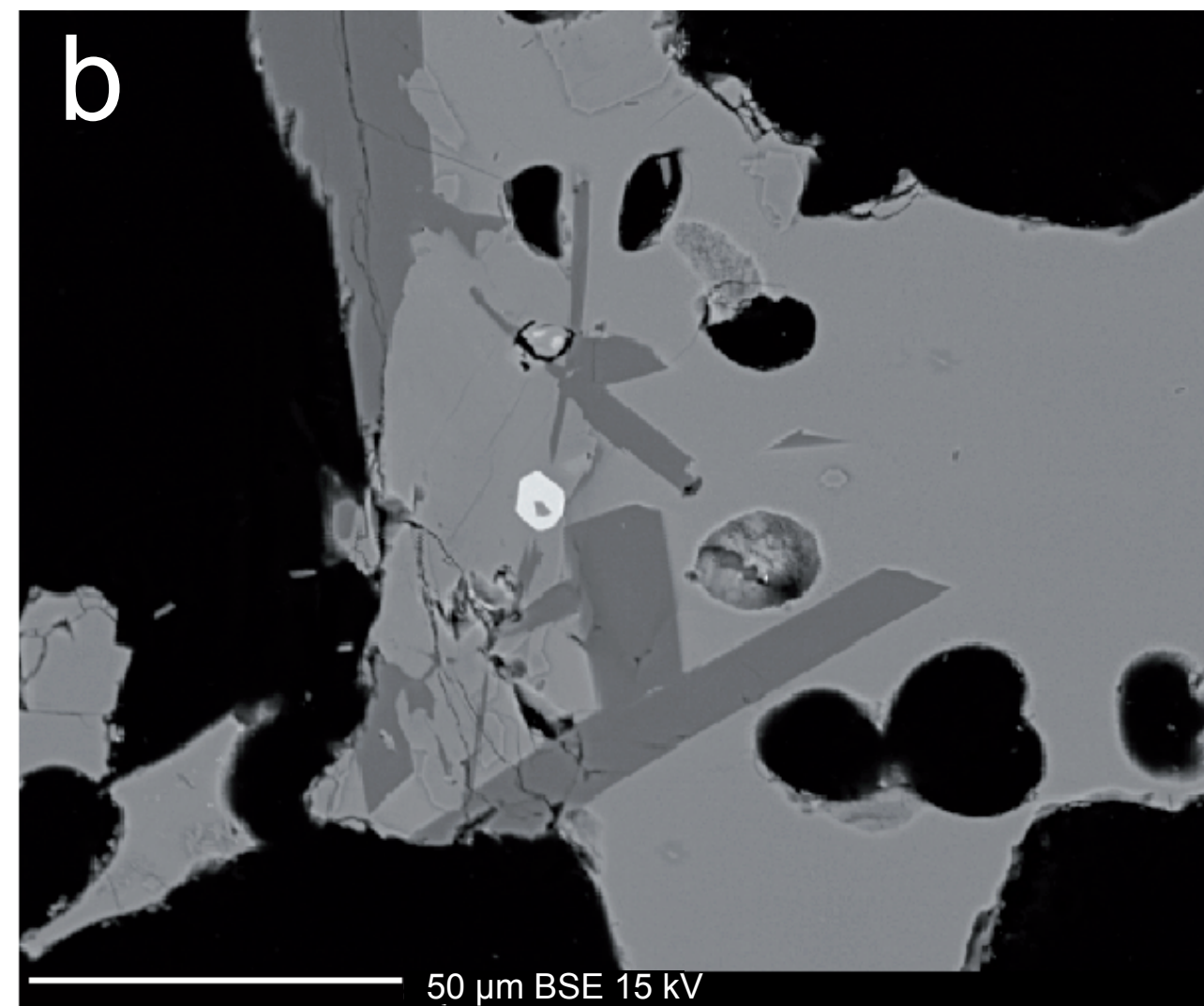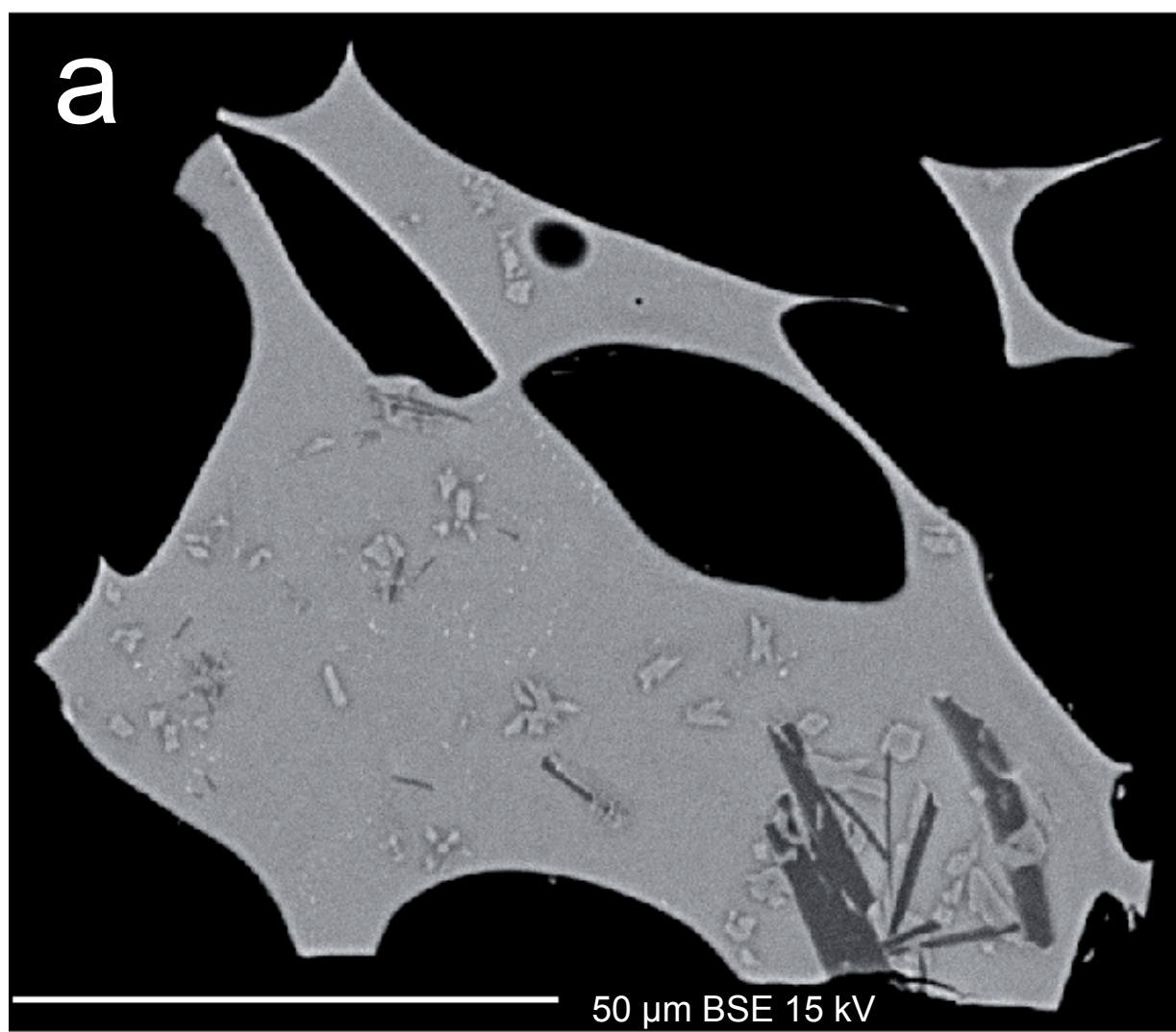
Figure legend

Fig.1   Back-scattered electron images of: a) phenocryst-poor but microlite-rich glass; b) phenocryst-rich tephra grain with euhedral plagioclase, clinopyroxene and titanomagnetite in a microlite-free glass; c) sulfide globule in tephra Gv2011-D. Melt inclusion in clinopyroxene is shown in panel d.
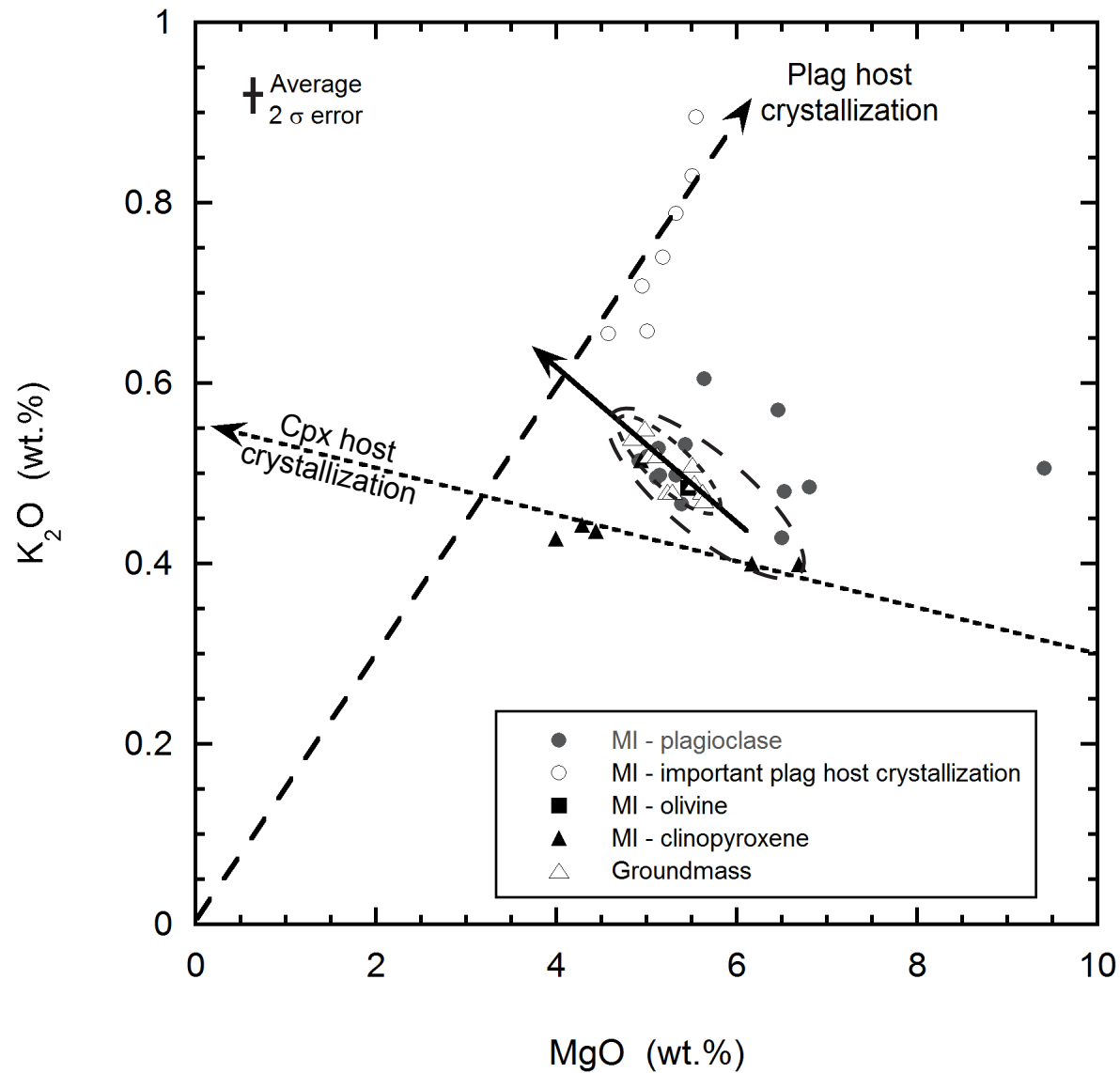
Fig.2   Variations of S, MgO and K_2O concentrations (in weight %) in melt inclusions (MI) and groundmass glass in tephra samples Gv2011-D and GV-4. a) Groundmass glass compositions form a linear array ($R^2 = 0.71$) upon which MI in olivine and several MI in plagioclase plot. Other plagioclase (plag) MI are subject to host crystallization as shown by a vector extending from the plag composition at the origin. Same holds for MI plotting above the groundmass glass array. Three MI in clinopyroxene (cpx) with lowest MgO concentration lie on a vector from the cpx composition passing through the most primitive cpx MI. b) Initial S concentration is estimated by extrapolating the K_2O concentrations measured in the most primitive cpx MI along the melt differentiation vector towards the groundmass value (from 0.4 to 0.5% yielding initial S of 1750 ppm). This value is indistinguishable from that measured in the most primitive plag MI (1772 ppm) and close to the average cpx MI value (1558 ppm; see text for further discussion). The vertical arrow indicates sulfur decrease caused by combined basalt-sulfide melt immiscibility and sulfur degassing.

Fig.3   Aura/OMI measurements of SO_2 column amounts in the Grímsvötn eruption cloud on (a) May22; (b) May 23; (c) May 24. Volcanic ash is indicated by positive values of the UV Aerosol Index. Note the distinct separation of tropospheric ash and stratospheric SO_2, due to strong   vertical   wind   shear.   Triangle   indicates   the   location   of   Grímsvötn.

Table 1. Calculation of S budget in Grímsvötn 2011 eruption*

	m(S)	S satellite	S leachate	S lake	S globules	α	ρ (density)	V_{DRE}	S(initial)	S(groundmass)
Values	0.73 Tg	0.19 Tg	0.12 Tg	0.037 Tg	0.38 Tg	1.998	2750 kg.m^{-3}	0.25 km^3	0.1750 wt%	0.0687 wt%
Errors	± 25%	± 30%	± 30%	± 30%	± 51%	---	± 2%	± 20%	± 7%	± 14%
		Contribution to the SO$_2$ budget								
mean m(SO$_2$)	1.47 Tg	0.38 Tg (26%)	0.24 Tg (16%)	0.07 Tg (5%)	0.78 Tg (53%)					
min m(SO$_2$)	1.10 Tg	0.38 Tg (35%)	0.24 Tg (22%)	0.07 Tg (6%)	0.41 Tg (37%)					
max m(SO$_2$)	1.82 Tg	0.38 Tg (17%)	0.24 Tg (11%)	0.07 Tg (3%)	1.13 Tg (62%)					

*m(S) and m(SO$_2$): total masses of S and SO$_2$, respectively, exsolved during the Grímsvötn 2011 eruption; α = MW(SO$_2$) / MW(S); DRE: Dense Rock Equivalent.

m(SO$_2$) = α x m(S); m(S) = ρ x V_{DRE} x (S(initial)-S(groundmass)).

(a)

(b)

SO$_2$ column TRM [DU]   UV Aerosol Index

1.0   2.0   3.0   4.0   5.0   6.0   2.0   2.6   3.2   3.8   4.4   5.0

(c)

Figure 3.

Auxiliary material for ms#2013g1057760

The sulfur budget of the 2011 Grímsvötn eruption, Iceland.
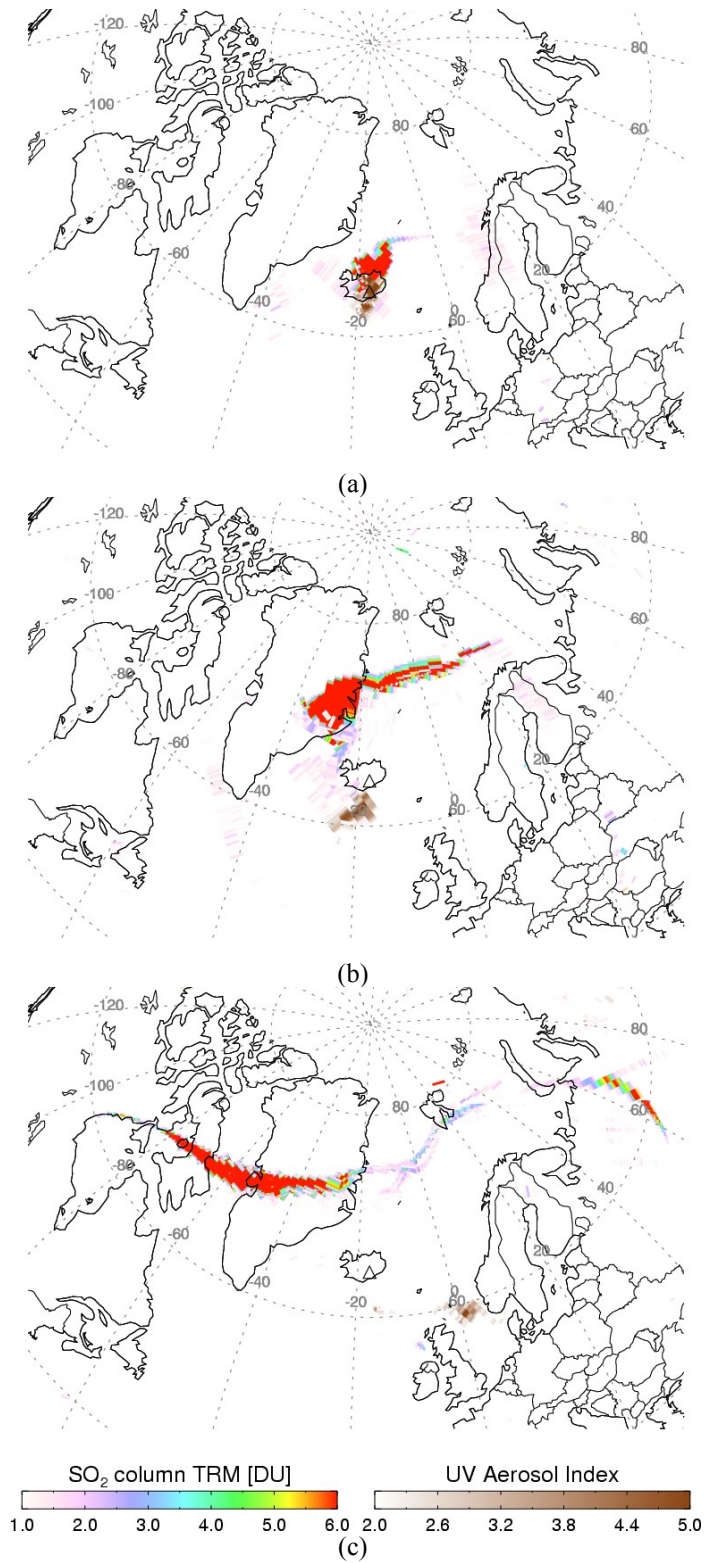
Olgeir Sigmarsson[1,2], Baptiste Haddadi[1], Simon Carn[3], Séverine Moune[1], Jónas Gudnason[2], Kai Yang[4,5] and Lieven Clarisse[6]

[1]LMV, CNRS-UBP-IRD, 5 rue Kessler, 63038 Clermont-Ferrand, France
[2]ISE, University of Iceland, 101 Reykjavik, Iceland
[3]Dept Geo Min Eng Sci, MTU, 1400 Townsend Drive, Houghton, MI 49931, USA
[4]Atmospheric Chemistry and Dynamics Laboratory, Code 614, NASA Goddard Space Flight Center, 8800 Greenbelt Rd Greenbelt, MD 20771, USA
[5]Dept of Atmospheric and Oceanic Science, University of Maryland College Park, College Park, MD 20742, USA
[6] Spectroscopie de l'Atmosphère, Service de Chimie Quantique et Photophysique, Université Libre de Bruxelles, Brussels, Belgium

Introduction

This data set contains the electron microprobe analysis of both melt inclusions and the groundmass glass (see "ts01.xlsx") of bulk tephra from the Grímsvötn 2011 eruption. For comparison, the groundmass glass S contents of earliest emitted tephra are given in "ts02.xlsx".

1. ts01.xlsx
1.1 Column "Object", type of object analyzed.
1.2 Column "Sample name", name of the object analyzed.
1.3 Column "SiO_2", SiO_2 concentration in weight percent of the object analyzed.
1.4 Nine following columns: concentration in weight percent of the oxide in the title of the column.
1.5 Column "S", S concentration in weight percent of the object analyzed, the sulfur speciation being taken for account.
1.6 Column "Sum", sum of the concentrations of the eleven precedent columns.
1.7 Column "S-error (2σ)", two sigma error on values in column "S".
1.8 Column "S-error (%, 2σ)", two sigma relative error on values in column "S".

2. ts02.xlsx
2.1 Column "Sample", name of the sample analyzed.
2.2 Column "S (wt%)", S concentration in weight percent of different glasses, the sulfur speciation being taken for account.
2.3 Column "$\pm 2\sigma$", two sigma error on values in column "S (wt%)".
2.4 Column "%, $\pm 2\sigma$", two sigma relative error on values in column "S (wt%)".

This table presents the data used to create the figures 2a and 2b.

Object	Sample name	SiO$_2$	TiO$_2$	Al$_2$O$_3$	FeO^{tot}	MnO	MgO	CaO	Na$_2$O	K$_2$O	P$_2$O$_5$	S	Sum	S-error (2σ)	S-error (%, 2σ)
MI in plag.	G1-A1	48.12	3.43	11.83	15.93	0.301	5.51	9.19	2.41	0.830	0.736	0.1982	98.5	0.0180	9.1
	G1-A2	49.56	3.45	10.49	16.37	0.326	5.55	8.83	2.16	0.895	0.484	0.1820	98.3	0.0150	8.2
	G1-C1	50.77	3.50	10.63	15.48	0.258	5.33	8.45	2.22	0.788	0.319	0.1726	97.9	0.0138	8.0
	G1-D1	52.05	1.57	12.49	9.93	0.223	9.41	9.67	2.48	0.506	0.073	0.1170	98.5	0.0098	8.4
	G1-E1	48.78	3.10	13.03	13.80	0.281	5.33	9.92	2.68	0.498	0.398	0.1698	98.0	0.0120	7.1
	G1-E2	49.06	2.89	12.94	13.45	0.181	5.15	9.75	2.68	0.498	0.323	0.1513	97.1	0.0126	8.3
	G1-E3	49.68	2.94	12.95	13.90	0.079	5.11	9.79	2.54	0.495	0.279		97.8		
	G1-F1	48.27	2.73	12.59	14.96	0.299	5.01	9.51	2.64	0.658	0.287	0.1617	97.1	0.0224	13.9
	G1-G1	50.55	2.43	13.00	12.83	0.204	6.50	10.08	2.62	0.429	0.233	0.1772	99.0	0.0116	6.5
	G1-G2	50.29	2.28	12.43	13.76	0.239	6.81	9.72	2.41	0.485	0.128	0.1640	98.7	0.0098	6.0
	G1-G3	50.78	2.49	13.36	13.29	0.253	6.53	10.05	2.62	0.480	0.256	0.1830	100.3	0.0140	7.7
	G1-H1	50.28	3.27	13.18	14.34	0.212	5.01	9.18	2.79	0.519	0.231	0.1664	99.2	0.0132	7.9
	G2-B1	48.60	2.59	12.72	14.21	0.355	5.18	9.05	2.65	0.740	0.231	0.1827	96.5	0.0116	6.3
	G2-B2	50.29	2.15	12.64	13.69	0.331	4.95	8.85	2.80	0.708	0.144	0.1663	96.7	0.0138	8.3
	G2-C1	49.43	2.39	13.59	14.65	0.271	4.58	9.55	2.82	0.655	0.263	0.1698	98.4	0.0128	7.5
	G2-D1	50.35	3.26	13.13	14.37	0.145	5.13	9.54	2.90	0.528	0.295	0.1706	99.8	0.0140	8.2
	G2-E1	52.15	2.57	13.09	12.02	0.241	6.46	9.56	3.00	0.570	0.288	0.1417	100.1	0.0130	9.2
	G2-F1	49.63	2.88	12.84	14.03	0.176	5.39	9.26	2.68	0.466	0.315	0.1834	97.9	0.0076	4.1
	G2-F2	49.55	2.82	12.86	14.47	0.149	5.64	8.74	2.68	0.605	0.320	0.1836	98.0	0.0178	9.7
	G2-G1	50.12	2.30	11.48	15.08	0.280	5.43	9.69	2.16	0.532	0.191	0.1619	97.4	0.0118	7.3
	G2-G2	49.83	1.98	13.33	13.86	0.155	4.92	9.95	2.72	0.514	0.072	0.1489	97.5	0.0126	8.5
MI in cpx.	G3-A1	49.88	2.87	14.43	13.14		4.94	9.18	2.76	0.515	0.352	0.1722	98.4	0.0088	5.1
	G3-B1	49.55	2.42	14.77	11.42	0.278	6.17	10.34	2.54	0.400	0.366	0.1313	98.4	0.007	5.3
	G3-B2	50.19	2.25	14.21	11.52	0.296	6.69	10.81	2.57	0.399	0.215	0.1308	99.3	0.0112	8.6
	G3-C1	49.75	2.95	14.17	14.14	0.201	4.44	8.84	2.68	0.436	0.342	0.1623	98.2	0.0162	10.0
	G3-E1	52.07	3.14	14.00	13.12	0.334	4.29	8.70	2.30	0.443	0.256	0.1858	99.0	0.0096	5.2
	G3-F1	51.40	2.54	15.66	13.39		3.99	8.30	2.50	0.428	0.321	0.1522	98.7	0.015	9.9
MI in ol.	G1-B1	50.84	2.75	13.59	13.88	0.197	5.46	9.89	2.98	0.484	0.251	0.1457	100.5	0.0090	6.2
GG.	#10/27	49.72	2.89	13.50	12.89	0.172	5.53	9.91	2.84	0.486	0.278	0.0543	98.3	0.0084	15.5
	#11/24	50.04	2.80	13.66	12.48	0.205	5.51	9.90	2.76	0.512	0.259	0.0708	98.2	0.0018	2.5
	#12/25	49.49	3.27	12.90	14.24	0.221	5.08	9.26	2.58	0.522	0.298	0.0750	97.9	0.0026	3.5
	#13/26	49.24	2.75	13.64	12.65	0.278	5.62	9.88	2.79	0.481	0.262	0.0876	97.7	0.0086	9.8
	#14/28	49.85	3.21	13.13	14.12	0.307	4.84	9.03	2.87	0.540	0.385	0.0779	98.4	0.0096	12.3
	#16/29	49.88	3.17	13.14	13.88	0.111	4.98	9.13	2.71	0.546	0.364	0.0826	98.0	0.0086	10.4
	#18/30	49.30	3.30	12.85	13.74	0.179	5.03	9.22	2.82	0.520	0.406	0.0895	97.5	0.0074	8.3
	#19/31	49.69	2.72	13.52	12.59	0.156	5.63	10.04	2.91	0.472	0.287	0.0627	98.1	0.0042	6.7
	#20/32	49.18	2.86	13.54	13.11	0.164	5.23	9.64	2.81	0.484	0.355	0.0465	97.4	0.0044	9.5
	#21/33	49.69	3.04	13.51	13.85	0.203	5.12	9.55	2.57	0.524	0.420	0.0502	98.5	0.0076	15.1
	#22/34	49.31	2.86	13.63	13.09	0.284	5.29	9.76	2.57	0.482	0.359	0.0537	97.7	0.0038	7.1

Each S concentration value is the mean of five individual measures on the same glass spot. Errors on S concentration are 2 standard deviation around the mean.
Abbreviations are: MI : melt inclusion; FeO^{tot}: total iron as FeO; plag: plagioclase; cpx: clinopyroxene; ol: olivine; GG: groundmass glass.
Sample name "G1-A2" corresponds to melt inclusion #2 in crystal A of group #1.
Sample name "#10/27" corresponds to glass analysis #10 and S concentration analysis #27.

Additional groundmass glass sulfur concentrations of the Grímsvötn 2011 eruption.

Sample	S (wt%)	±2σ	%, ±2σ
GV-1	0.0469	0.0017	3.6
	0.0569	0.0074	13.0
	0.0539	0.0045	8.3
	0.0660	0.0066	10.0
GV-2	0.0853	0.0054	6.3
	0.0618	0.0081	13.2
	0.0620	0.0059	9.4
	0.0636	0.0059	9.2
	0.1034	0.0145	14.0
GV-3	0.0449	0.0043	9.5
	0.0698	0.0113	16.2
	0.0521	0.0030	5.8
	0.0752	0.0124	16.5
	0.0673	0.0046	6.8

Each S concentration value is the mean of five individual measures on the same glass spot.
Errors on S concentration are 2 standard deviation around the mean.
Abbreviation is: wt% for weight percentage.